HHS Public Access

Author manuscript

Connect Tissue Res. Author manuscript; available in PMC 2019 December 01.

Published in final edited form as:

Connect Tissue Res. 2018 December ; 59(SUP1): 30–34. doi:10.1080/03008207.2017.1408602.

Pleiotropic function of DLX3 in amelogenesis: from regulating pH and keratin expression to controlling enamel rod decussation

Olivier Duverger[1,*] and **Maria I. Morasso**[1]

[1]Laboratory of Skin Biology, National Institute of Arthritis and Musculoskeletal and Skin Diseases, National Institutes of Health, Bethesda, MD, USA

Abstract

DLX3 is essential for tooth enamel development and is so far the only transcription factor known to be mutated in a syndromic form of amelogenesis imperfecta. Through conditional deletion of *Dlx3* in the dental epithelium in mouse, we have previously established the involvement of DLX3 in enamel pH regulation, as well as in controlling the expression of sets of keratins that contribute to enamel rod sheath formation. Here, we show that the decussation pattern of enamel rods was lost in conditional knockout animals, suggesting that DLX3 controls the coordinated migration of ameloblasts during enamel secretion. We further demonstrate that DLX3 regulates the expression of some components of myosin II complexes potentially involved in driving the movement of ameloblasts that leads to enamel rod decussation.

Introduction

During tooth development, enamel is produced by epithelial-derived ameloblasts through a complex multi-step process called amelogenesis. Going through the stages of pre-secretion, secretion and maturation, ameloblasts build highly mineralized rods that are separated by interrod enamel.

Mutations in the gene encoding the homeodomain transcription factor DLX3 lead to tricho-dento-osseous (TDO) syndrome, an ectodermal dysplasia characterized by anomalies in hair, teeth and bone development (1). Dental defects in TDO patients include severe enamel hypoplasia and hypomineralization. We previously showed that conditional deletion of *Dlx3* in the dental epithelium in mice recapitulates these enamel defects (2). Through transcriptomic analyses, we demonstrated that DLX3 is required for the expression of carbonic anhydrases and ion transporters that are essential regulators of pH during enamel maturation (2). Moreover, we determined that specific sets of keratins regulated by DLX3 are expressed by ameloblasts and incorporated into the enamel where they play a crucial role in enamel rod sheath formation and in the resistance to caries (3).

Enamel rods exhibit a very intricate arrangement called rod decussation. This pattern contributes to the unique biomechanical properties of enamel and is the product of a

*Address correspondence to: duvergero@mail.nih.gov (OD).

The authors have declared that no conflict of interest exists

coordinated movement of rows of ameloblasts during the secretion phase. Even though the cellular mechanisms controlling this process have been proposed to involve cytoskeletal components, planar cell polarity and intercellular junctions (4–6), as well as matrix metalloprotease activity (7, 8), the specific mechanism that drive the coordinated movement of the cells have not been determined.

Here we describe an additional function for DLX3 during the secretory stage of amelogenesis that implicates specific components of a myosin II motor mechanism into the cellular process that drives the formation of enamel rod decussation.

Results

Enamel rod decussation is impaired in Dlx3$^{K14\text{-}cKO}$ mice.

We recently showed that conditional deletion of *Dlx3* in the dental epithelium leads to the formation of hypomineralized enamel that gets eroded after tooth eruption *(2)*. Detailed analysis of the enamel structure using scanning electron microscopy on a portion of the continuously growing incisor protected by alveolar bone, revealed that the characteristic decussation pattern of enamel rods was lost in *Dlx3*$^{K14\text{-}cKO}$ mice (Figure 1A). This observation was corroborated by histological analysis of secretory-stage ameloblasts observed on a cross section of the continuously erupting incisor, which revealed that ameloblasts in *Dlx3*^{WT} mice appear intertwined while they are arranged in parallel in *Dlx3*$^{K14\text{-}cKO}$ mice (Figure 1B). Moreover, the enamel matrix exhibits a lattice pattern in *Dlx3*^{WT} mice that is not seen in Dlx3$^{K14\text{-}cKO}$ mice (Figure 1B**, insets**). These observations indicate that DLX3 is required for enamel rod decussation.

DLX3 controls the expression of myosin II subunits and associated proteins.

Using RNA-seq, we identified genes affected by the absence of DLX3 in the enamel organ. We reported previously that the expression of *Mmp20* was not affected significantly in the enamel organ of *Dlx3*$^{K14\text{-}cKO}$ mice *(2)*, suggesting that the loss of decussation pattern in our mouse model may not be the result of impaired modulation of cell-cell junctional complexes due to the absence of the matrix metalloprotease MMP20 (7, 8). Moreover, no effect was detected on the expression of components of cell-cell junction complexes (adherens junctions, tight junctions), except for a moderate decrease in desmoglein 2 expression (Dsg2, FC=−1.49). Also, elements of planar cell polarity (*Vangl1, Prickle1, Prickle2*) were unaffected.

However, the expression of several genes endoding myosin II subunits and associated proteins was affected significantly in the enamel organ of *Dlx3*$^{K14\text{-}cKO}$ mice (Table 1 **and** Figure 2A). The expression of myosin heavy chain 4 (*Myh4*) was decreased while the expression of myosin light chain 4 (*Myl4*) was increased. Interestingly, both of these myosins are known as being muscle-specific, with *Myl4* expression being restricted to embryonic muscle. The mRNA level of the regulatory myosin light chain subunit 12b (*Myl12b*), that presents a much higher expression than *Myh4* and *Myl4* (Figure 2A), exhibited a mild but significant decrease in the enamel organ of *Dlx3*$^{K14\text{-}cKO}$ mice. Considering proteins that are involved in the regulation of myosin II activity through

phosphorylation, myosin light chain kinase 3 (*Mylk3*) was also downregulated significantly in the absence of DLX3. Finally, the expression of subunit 1 of troponin I (*Tnni1*), a protein involved in the interaction between myosin II and actin, was upregulated.

We further determined that several non-muscle myosin heavy chains (*Myh9, Myh10, Myh11* and *Myh14*) and myosin light chains (*Myl6* and *Myl9*), that are unaffected by *Dlx3* deletion, were highly expressed in the enamel organ (Figure 2B). Among myosin associated proteins, all tropomyosins were highly expressed and several troponins were detected in the enamel organ (Figure 2B).

These findings indicate that DLX3 controls part of an actinomyosin machinery involved in the coordinated movement of ameloblasts, a mechanism that has previously been proposed (4–6).

The distribution pattern of myosin heavy chains is altered in ameloblasts from Dlx3$^{K14\text{-}cKO}$ mice.

To assess the effect of *Dlx3* deletion on the overall distribution of myosin complexes, we performed immunohistochemical staining of myosin heavy chains in the enamel organ of *Dlx3*^{WT} and *Dlx3*$^{K14\text{-}cKO}$ mice, using an antibody that recognizes all subunits. Myosin heavy chain staining was restricted to ameloblasts and distribution was altered in *Dlx3*$^{K14\text{-}cKO}$ mice, with accumulation of complexes in areas of the ameloblast layer (Figure 2C). These observations suggest that the changes in expression of myosin II subunits and associated proteins due to the absence of DLX3 result in defective myosin II complex assembly and localization, preventing proper migration of ameloblasts during enamel secretion.

Discussion

Myosin II has been implicated in various developmental processes that require the coordinated movement of epithelial cells in the early embryo and in developing or regenerating tissues (9–11). The intricate pattern of enamel rods also involves the coordinated movement of ameloblasts during the secretion stage of enamel formation. Although it has been suggested that this process involves an actinomyosin mechanism (4–6), this hypothesis has not been verified.

Here we determine that the transcription factor DLX3 is required for proper enamel rod decussation, and that several subunits of myosin II and associated proteins are regulated by DLX3 in the enamel organ. While *Myl4* expression is upregulated, the expression of *Myh4* and *Myl12b* decreases, which suggests a complex regulation process where DLX3 may repress or upregulate specific myosin II subunits, in a direct or indirect manner. Interestingly, *Myh4* and *Myl4* are known to be muscle-specific, while *Myl12b* is found both in smooth muscle and non-muscle tissues. Moreover, several other non-muscle subunits of myosin II are expressed in the enamel organ. These results reveal that the enamel organ expresses a combination of muscle-specific and non-muscle myosin II subunits. Our immunohistochemical analysis further determines that myosin heavy chains are restricted to the ameloblast layer of the enamel organ. Moreover, to support our hypothesis that the

disruption of the myosin II motor machinery is likely to be responsible for the loss of decussation pattern in $Dlx3^{K14\text{-}cKO}$ mice, we show that the overall distribution of myosin heavy chains is abnormal in ameloblasts lacking DLX3. We believe this disrupted pattern is due to altered expression of a subset of myosin II subunits, as well as defective functional regulation caused by decreased *Mylk3* expression.

Future studies will focus on dissecting the function of individual subunits by precise immunolocalization, as well as genetic and pharmacological manipulation. Concerning the function of DLX3 in amelogenesis, these findings further highlight the pleiotropic function of a single transcription factor in the control of complex molecular and cellular events that lead to tooth enamel formation.

Materials and Methods

Mice.

K14-cre mice were mated with $Dlx3^{Flox/Flox}$ mice to generate $Dlx3^{K14\text{-}cKO}$ mice, as described previously (2). All animal work was approved by the Animal Care and Use Committee of the NIAMS (ASP #A016-08-02 for M.I.M.).

Scanning electron microscopy.

Mandibles from 8-week old mice were embedded in acrylic and sectioned using an Isomet slow-speed diamond saw (Buehler, Lake Bluff, IL, USA) in a plane perpendicular to the axis of the incisor at the level of the first molar (distal side). Sections were grinded using 1200 grit sandpaper using an EcoMet™ 250 (Buehler), polished on diamond lapping film up to 0.1 μm, etched with 37% phosphoric acid for 10 seconds, and sonicated. Sections were then prepared for scanning electron microscopy as described previously (2) and analyzed under a Field Emission Scanning Electron Microscope S4800 (Hitashi, Toronto, Canada) at 10 kV.

Histology.

Heads from 5-day old mice were fixed in 4% PFA, decalcified and embedded in paraffin. 10 μm coronal sections were made to obtain cross sections of the continuously growing incisors. Hematoxylin and eosin staining was performed using standard procedure.

RNA-seq analysis.

RNA-seq was performed on enamel organ dissected from four $Dlx3^{WT}$ and four $Dlx3^{K14\text{-}cKO}$ mice at postnatal day 10, as described previously (2), using the HiSeq® 2500 (Illumina, San Diego, CA). The data has been deposited to the Gene Expression Omnibus site (Accession number: GSE57984). Partek Genomics Suite (http://www.partek.com) was used for statistical analysis and fold-changes calculation.

Immunohistochemistry.

Immunohistochemical analysis was performed on 10 μm sections from 4% PFA-fixed and paraffin-embedded rat mandibles using anti-MHC (MF-20, deposited to DSHB by Fischman, D.A.). Anti-mouse IgG conjugated to Alexa Fluor 488 was used as a secondary

antibody. DAPI was used to stain nuclei. Image acquisition was performed on a Leica SP5 confocal microscope.

Acknowledgements

We thank the Next Generation Sequencing core facility, the Biodata Mining core facility, and the Light Imaging core facility of the NIAMS. We thank Dr. Richard Leapman from the NIBIB for giving us access to their equipment for scanning electron microscopy analysis. This work was supported by the intramural research program of the National Institute of Arthritis and Musculoskeletal and Skin Diseases (M.I.M. AR041171).

References

1. Price JA, Bowden DW, Wright JT, Pettenati MJ, Hart TC. Identification of a mutation in DLX3 associated with tricho-dento-osseous (TDO) syndrome. Hum Mol Genet. 1998;7(3):563–9. [PubMed: 9467018]
2. Duverger O, Ohara T, Bible PW, Zah A, Morasso MI. DLX3-Dependent Regulation of Ion Transporters and Carbonic Anhydrases is Crucial for Enamel Mineralization. J Bone Miner Res. 2017;32(3):641–53. [PubMed: 27760456]
3. Duverger O, Ohara T, Shaffer JR, Donahue D, Zerfas P, Dullnig A, Crecelius C, Beniash E, Marazita ML, Morasso MI. Hair keratin mutations in tooth enamel increase dental decay risk. J Clin Invest. 2014;124(12):5219–24. [PubMed: 25347471]
4. Nishikawa S Correlation of the arrangement pattern of enamel rods and secretory ameloblasts in pig and monkey teeth: a possible role of the terminal webs in ameloblast movement during secretion. Anat Rec. 1992;232(4):466–78. [PubMed: 1554099]
5. Nishikawa S Cytoskeleton, intercellular junctions, planar cell polarity, and cell movement in amelogenesis. Journal of Oral Biosciences. 2017;59(4):197–204.
6. Nishikawa S, Fujiwara K, Kitamura H. Formation of the tooth enamel rod pattern and the cytoskeletal organization in secretory ameloblasts of the rat incisor. Eur J Cell Biol. 1988;47(2): 222–32. [PubMed: 3149586]
7. Bartlett JD, Skobe Z, Nanci A, Smith CE. Matrix metalloproteinase 20 promotes a smooth enamel surface, a strong dentino-enamel junction, and a decussating enamel rod pattern. Eur J Oral Sci. 2011;119 Suppl 1:199–205. [PubMed: 22243247]
8. Bartlett JD, Smith CE. Modulation of cell-cell junctional complexes by matrix metalloproteinases. J Dent Res. 2013;92(1):10–7. [PubMed: 23053846]
9. Rozbicki E, Chuai M, Karjalainen AI, Song F, Sang HM, Martin R, Knolker HJ, MacDonald MP, Weijer CJ. Myosin-II-mediated cell shape changes and cell intercalation contribute to primitive streak formation. Nat Cell Biol. 2015;17(4):397–408. [PubMed: 25812521]
10. Vicente-Manzanares M, Ma X, Adelstein RS, Horwitz AR. Non-muscle myosin II takes centre stage in cell adhesion and migration. Nat Rev Mol Cell Biol. 2009;10(11):778–90. [PubMed: 19851336]
11. Wilson CA, Tsuchida MA, Allen GM, Barnhart EL, Applegate KT, Yam PT, Ji L, Keren K, Danuser G, Theriot JA. Myosin II contributes to cell-scale actin network treadmilling through network disassembly. Nature. 2010;465(7296):373–7. [PubMed: 20485438]

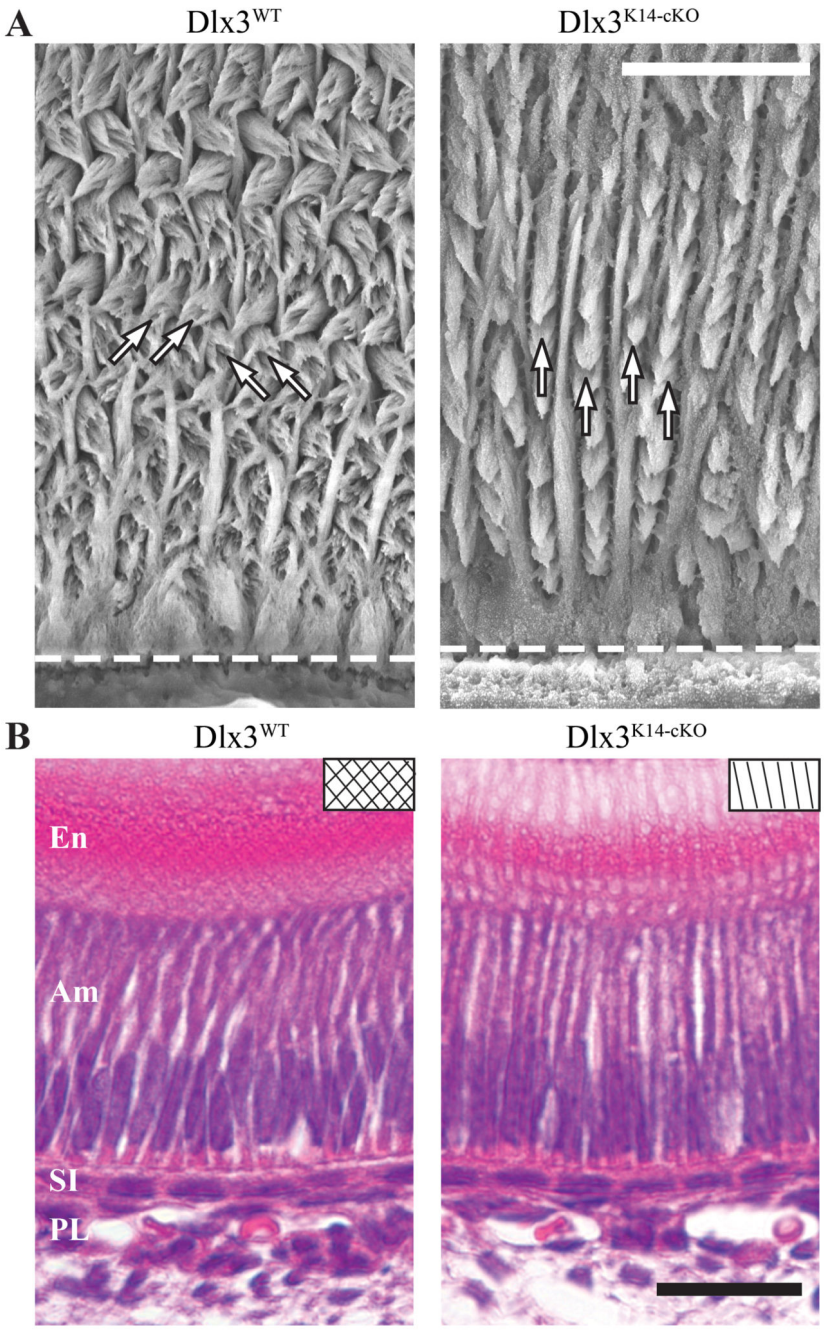

Figure 1: Loss of enamel rod decussation pattern in *Dlx3*$^{K14\text{-}cKO}$ mice.

(**A**) Scanning electron microscopy of enamel from *Dlx3*^{WT} and *Dlx3*$^{K14\text{-}cKO}$ mice at 8 weeks. White arrows indicate the orientation of enamel rods. The dashed line indicates the dentin-enamel junction. Scale bar: 10 μm. (**B**) Hematoxylin and Eosin staining of cross sections of mandibles from *Dlx3*^{WT} and *Dlx3*$^{K14\text{-}cKO}$ mice at postnatal day 5 showing the histology of secretory-stage ameloblasts (Am) and the pattern of the enamel matrix (En). Insets depict the pattern of the enamel matrix and show loss of the lattice pattern in *Dlx3*$^{K14\text{-}cKO}$ mice. SI, stratum intermedium; PL, papillary layer. Scale bar: 50 μm.

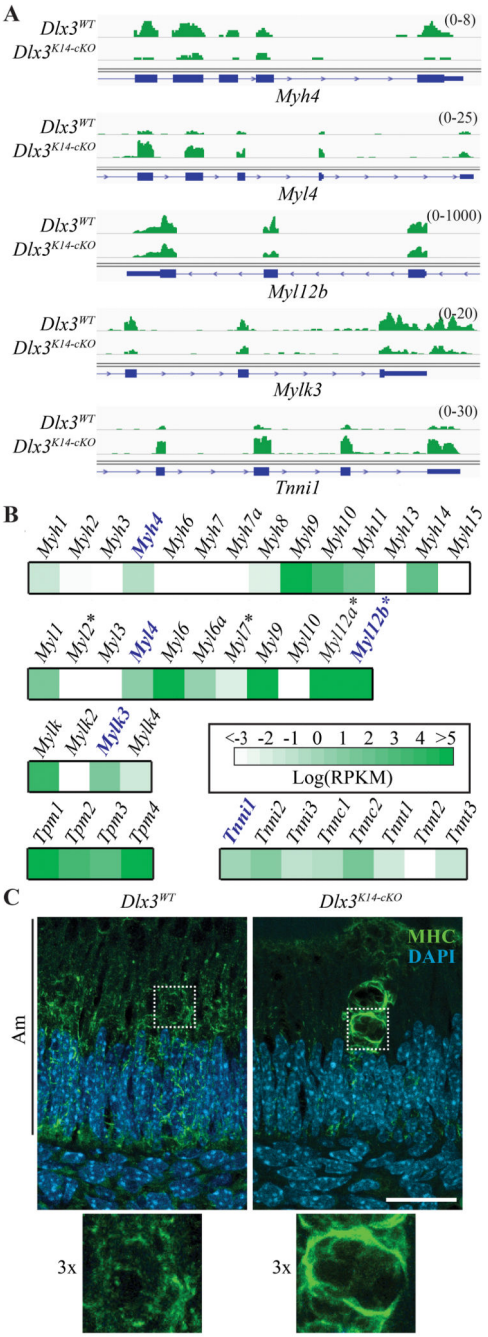

Figure 2: Effect of *Dlx3* deletion on the expression of myosin II subunits and associated proteins in the enamel organ.

(**A**) RNA-seq coverage data showing altered mRNA levels for *Myh4, Myl4, Myl12b, Mylk3 and Tnni1* in the enamel organ from *Dlx3*$^{K14\text{-}cKO}$ mice. (**B**) Heat maps indicating the expression level of all myosin heavy chain subunits (*Myh*), myosin light chain subunits (*Myl*, asterisks mark regulatory subunits), myosin light chain kinases (*Mylk*), tropomyosins (*Tpm*) and troponins (*Tnn*) in the enamel organ, based on Log-RPKM values. Transcripts affected by *Dlx3* deletion are in bold font. (**C**) Immunohistochemical detection of myosin

heavy chains (MHC, green) in the enamel organ of $Dlx3^{WT}$ and $Dlx3^{K14\text{-}cKO}$ mice at postnatal day 5 using an antibody recognizing all subunits. Bottom panels show inset magnification. Nuclei are stained with DAPI (blue). Am, ameloblasts. Scale bar: 20 μm.

Table 1:

Transcripts encoding myosin II subunits and associated proteins affected by *Dlx3* deletion in the enamel organ based on RNA-seq analysis.

Gene Symbol	Transcript (NM_)	p_value (cko vs. wt)	q_value (ko vs. wt)	FC (cko vs. wt)
Myh4	010855	0.011	0.123†	−5.35
Mylk3	175441	1.8E-05	0.006	−2.57
Myl12b	023402	3.7E-04	0.030	−1.24
Myl4	010858	0.001	0.041	3.65
Tnni1	021467	0.017	0.145†	6.45

Note: microarray analysis corroborated the changes presented here.

† q_value >0.05 but change confirmed by microarray.